Earthquakes and Structures, *Vol. 22, No. 4 (2022) 373-386*
https://doi.org/10.12989/eas.2022.22.4.373

An analytical model for displacement response spectrum considering the soil-resonance effect

Haizhong Zhang[a] and Yan-Gang Zhao*

Department of Architecture, Kanagawa University, Yokohama, Japan

(Received July 12, 2021, Revised March 29, 2022, Accepted April 6, 2022)

Abstract. The development of performance-based design methodologies requires a reasonable definition of a displacement-response spectrum. Although ground motions are known to be significantly affected by the resonant-like amplification behavior caused by multiple wave reflections within the surface soil, such a soil-resonance effect is seldom explicitly considered in current-displacement spectral models. In this study, an analytical approach is developed for the construction of displacement-response spectra by considering the soil-resonance effect. For this purpose, a simple and rational equation is proposed for the response spectral ratio at the site fundamental period (*SRTg*) to represent the soil-resonance effect based on wave multiple reflection theory. In addition, a bilinear model is adopted to construct the soil displacement-response spectra. The proposed model is verified by comparing its results with those obtained from actual observations and SHAKE analyses. The results show that the proposed model can lead to very good estimations of *SRTg* for harmonic incident seismic waves and lead to reasonable estimations of *SRTg* and soil displacement-response spectra for earthquakes with a relatively large magnitude, which are generally considered for seismic design, particularly in high-seismicity regions.

Keywords: displacement; response spectral ratio; response spectrum; site fundamental period; soil-resonance effect

1. Introduction

The performance-based design has been widely accepted in recent years as a more rational approach for structural seismic design. This is because the displacement-related parameters could better reflect the structural damage during the earthquakes than strength, in most cases. With the development of performance-based design approaches, a reasonable definition of the displacement-response spectrum has received increasing research attention (Calvi 2019, Devandiran *et al*. 2013, Muho *et al*. 2020). Early studies, e.g., Tolis and Faccioli (1999) and Bommer and Elnashnai (1999), pointed out that displacement spectra approximately converted from acceleration spectra specified in seismic codes are generally unrealistic, particularly within a long period range. Since then, researchers have focused on exploring more reasonable displacement spectral models. Tolis and Faccioli (1999) developed a displacement spectral model based on statistical analysis of the 1995 Kobe earthquake. Bommer and Elnashnai (1999) proposed a ground-motion prediction model for displacement spectral ordinates based on a dataset of European strong motions. The achievements of the two studies were incorporated into Eurocode 8 (2004) to formulate the design displacement spectrum. Subsequently, Akkar and Bommer (2007) presented another prediction equation for displacement response ordinates by using 532 accelerograms from the strong-motion databank from Europe and the Middle East. The aforementioned studies mainly discussed displacement spectra at periods shorter than 4 s. Faccioli *et al*. (2004) investigated long-period spectral ordinates by using digital recordings of various earthquakes from Japan, Italy, Greece, and Taiwan. Guan *et al*. (2004) developed a model considering the long-period range based on a ground-motion data-processing procedure using 541 records collected throughout the world. Cauzzi and Faccioli (2008) formulated an equation for the prediction of displacement spectral ordinates up to 20 s based on 60 earthquakes worldwide. In addition, Maniatakis and Spyrakos (2012) and Zhao *et al*. (2019) explored displacement spectral models for near-fault ground motions. Lumantarna *et al*. (2012) developed a bilinear rock displacement spectral model for engineering applications in low and moderate seismicity regions.

The surface ground motion is known to be significantly affected by local site conditions (Pitilakis *et al*. 2011, Manolis *et al*. 2013, Ranjan and Kumar 2021, Sisi *et al*. 2018), particularly the resonant-like amplification behavior caused by multiple wave reflections within the surface soil. The resonant-like amplification phenomenon does not necessarily require the consistency between the predominant period of the earthquake motion with the site fundamental period, but happens for general earthquake motions, which performs as the significant amplification of the components with periods near the site fundamental period caused by the resonance effect (Tsang *et al*. 2017). Although many displacement spectral models (Bommer and Elnashnai 1999, Akkar and Bommer 2007, Guan *et al*. 2004) have incorporated site effects based on site

*Corresponding author, Professor
E-mail: zhao@kanagawa-u.ac.jp
[a]Ph.D.
E-mail: zhang@kanagawa-u.ac.jp

http://www.techno-press.com/journals/eas&subpage=7
ISSN: 2092-7614 (Print), 2092-7622 (Online)

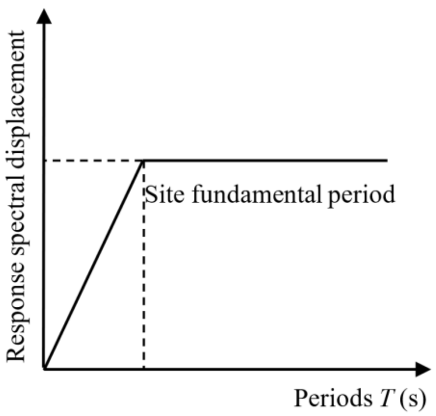

Fig. 1 Bilinear model for construction of the soil-displacement spectrum

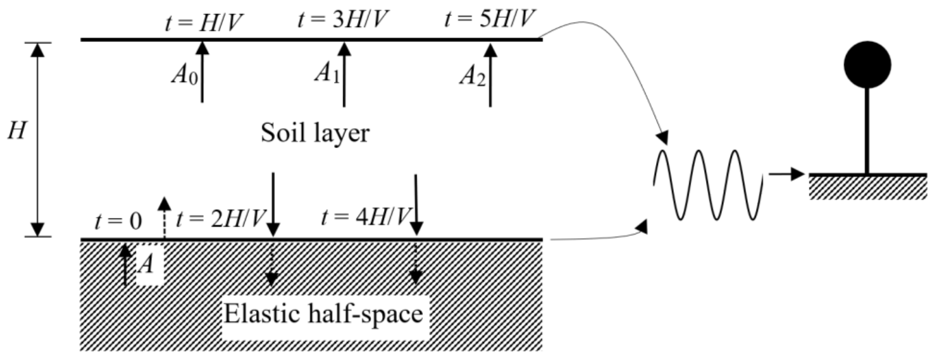

(a) A single-layer soil profile on elastic half-space for estimation of site effects

(b) A single-degree-of-freedom system for calculation of response spectra

Fig. 2 The simple models used for the analysis of the response spectral ratio

classification, the periodic soil-resonance effect has been seldom explicitly considered. To solve this problem, Lam *et al*. (2001) proposed a bilinear model for the displacement-response spectrum to incorporate the soil-resonance effect. The basic steps in the application of the model involve (i) the calculation of the soil displacement-response spectrum at the site fundamental period, and then (ii) the construction of the soil displacement-response spectrum at whole periods using two straight lines, as illustrated in Fig. 1. Tsang *et al*. (2006a) derived an approximate equation for the response spectral ratio at the site fundamental period (SR_{Tg}) to represent the soil-resonance effect based on the principle of the conservation of wave energy. Thus, the soil displacement-response spectrum at the site fundamental period can be obtained directly by multiplying SR_{Tg} with the bedrock displacement response spectrum at the site fundamental period. The Tsang equation considers the nonlinear behavior of soil and impedance contrast at the soil–bedrock interface. Subsequently, Tsang *et al*. (2017) further simplified the calculation of SR_{Tg} by replacing the equation with charts. These displacement spectral models are mainly developed for low-to-moderate seismicity regions; however, their applicability to high seismicity regions with large magnitude is poor, as described later.

This study aims to develop a new displacement spectral model considering the soil-resonance effect, which consists of developing a new equation for SR_{Tg} to represent the soil-resonance effect and using the bilinear model to construct the soil displacement-response spectra. The proposed model can provide a reasonable estimation of displacement spectra, for cases with a relatively large magnitude, which are generally considered for seismic design particularly in high-seismicity regions. The remainder of this paper is organized as follows. In Section 2, the response spectral ratio of a simple single-layer soil model subjected to harmonic incident waves is analyzed based on wave multiple reflection theory. Then, according to the analysis results, a simple equation for SR_{Tg} was proposed to represent the soil-resonance effect, and then a bilinear model was adopted to construct the soil displacement-response spectra. In Section 3, the proposed model is verified through comparisons with the results obtained from actual observations and the SHAKE program (Idriss and Sun 1992), considering recorded and synthetic earthquake motions as well as harmonic seismic waves. Finally, the conclusions are presented in Section 4.

2. Soil displacement spectral model

2.1 Response spectral ratio of a single-layer soil model

To obtain soil displacement-response spectra that consider the soil-resonance effect, the response spectral ratio of a single-layer soil profile on an elastic half-space, as shown in Fig. 2(a), subjected to an incident harmonic seismic wave is analyzed. Although the actual site can be multilayered or even more complex because of its three-dimensional nature, a single-layer soil model is widely used because of its ability to capture the main site characteristics and be easily understood. The incident wave is assumed to travel along a perfectly vertical path approaching the soil–bedrock interface, and its displacement as a function of time t is defined as

$$y(t) = Asin(\omega t) \tag{1}$$

where A and ω are the displacement amplitude and circular frequency of the incident wave, respectively.

To obtain the response spectral ratio of a single-layer soil model, the displacement of the ground surface should be derived first. According to the wave-propagation theory, when an incident wave with displacement amplitude A perpendicularly reaches the interface of two media, part of its energy is transmitted across the interface with displacement amplitude A_T, and the remaining energy is reflected back with displacement amplitude A_R. The displacement amplitudes of the transmitted and reflected waves can be obtained as follows:

$$T_r = \frac{A_T}{A} = \frac{2I}{1+I} \tag{2}$$

$$R_e = \frac{A_R}{A} = \frac{I-1}{I+1} \tag{3}$$

where T_r and R_e are the transmission and reflection coefficients, respectively, and I is the impedance ratio of the media wherein the incident and transmitted waves propagate. According to the definition of impedance ratio I, I should change depending on the direction of wave propagation, that is, from soil to rock or from rock to soil. For simplicity, impedance ratio I is defined as $\frac{\rho_B V_B}{\rho V}$ in this study and is independent of the wave-propagation direction. Here, ρ and V are the density and shear wave velocity of the soil layer, respectively; and ρ_B and V_B are the density and shear wave velocity of the bedrock, respectively. Thus, when the seismic wave is transmitted from the soil to bedrock, impedance ratio I in Eqs. (2) and (3) should be replaced by $1/I$. In addition, Eq. (3) indicates that when I is replaced by $1/I$, the absolute value of R_e remains unchanged but the sign becomes opposite.

According to Eq. (2), when the incident wave is transmitted across the soil–bedrock interface, as shown in Fig. 2(a), the amplitude reaches A_T and the polarity remains unchanged. The transmitted wave propagates upward and passes the soil layer, while the displacement amplitude is reduced because of viscous or hysteretic damping due to the nonlinear behavior of the soil layer. Tsang *et al.* (2006a) introduced a half-period damping ratio, β, to quantify the effect of soil damping for every half-period of wave travel.

$$\beta = exp(-\pi \mathrm{h}) \tag{4}$$

where h is the soil damping ratio. Specifically, when a seismic wave travels in a half-period, the amplitude will be reduced to β times the initial amplitude. Therefore, when the transmitted wave with period T ($T = 2\pi/\omega$) passes the soil layer once and reaches the ground surface after H/V seconds, it propagates $2H/(VT)$ half periods, and the displacement amplitude becomes

$$A_0 = \beta^{\frac{2H}{VT}} A_T = \beta^{\frac{T_g}{2T}} A_T \tag{5}$$

where H is the height of the soil layer, and T_g is the site fundamental period equal to $4H/V$. Compared with the incident wave at the soil–bedrock interface, the wave approaching the ground surface has an altered amplitude of A_0 and requires H/V seconds to reach the ground surface; thus, its displacement function $y_0(t)$ can be expressed as

$$y_0(t) = A_0 sin(\omega(t - H/V)) \tag{6}$$

Subsequently, the upward-propagating wave is reflected at the ground surface. Eq. (3) implies that when the wave reaches the ground surface, as shown in Fig. 2(a), the reflected wave has the same amplitude and polarity as the incident wave. Thus, the reflected wave from the ground surface will propagate downward with amplitude A_0. Considering the energy loss due to soil damping, the wave reaches the soil–bedrock interface with amplitude $\beta^{\frac{T_g}{2T}} A_0$ after H/V seconds. Similarly, the downward-propagating wave is reflected back from the soil–bedrock interface by the mechanism described earlier. Furthermore, Eq. (3) implies that when the wave propagates from the soft soil layer to the stiffer bedrock, the amplitude of the reflected wave is $|R_e|\beta^{\frac{T_g}{2T}} A_0$, and the polarity of the reflected wave is opposite to that of the incident wave. As $|R_e|$ is naturally lesser than 1, $|R_e|\beta^{\frac{T_g}{2T}} A_0$ would be lesser than $\beta^{\frac{T_g}{2T}} A_0$, indicating that the displacement amplitude is reduced every time the seismic wave is reflected by the stiffer bedrock. Essentially, the amplitude reduction is due to the energy loss at the soil–bedrock interface; this is known as radiation damping (Zhang and Zhao 2021c). Then, the reflected wave from the soil–bedrock interface propagates upward. Considering again the energy loss due to soil damping, the wave would reach the ground surface with amplitude $A_1 = |R_e|\beta^{\frac{T_g}{T}} A_0$ after another H/V seconds. Compared with the first seismic wave that reaches the ground surface ($t = H/V$), the seismic wave reflected back to the ground surface ($t = 3H/V$) showed a reduced amplitude of A_1, an opposite polarity, and reached the ground surface $2H/V$ seconds late. Thus, the displacement of the seismic wave reflected back to the ground surface, $y_1(t)$, can be expressed as

$$y_1(t) = -A_1 sin\big(\omega(t - 3H/V)\big) \tag{7}$$

The seismic wave continues to propagate and reflect at the soil–bedrock interface. Therefore, we conclude that when the seismic wave completes one round of propagation from the ground surface to the soil–bedrock interface and back to the ground surface, the amplitude is reduced to $|R_e|\beta^{\frac{T_g}{T}}$ times the previous amplitude, the polarity reverses, and t=$2H/V$ seconds pass. Therefore, the displacement of the i^{th} (i = 0, 1, 2…) seismic wave reflected back to the ground surface, $y_i(t)$, can be expressed as

$$y_i(t) = (-1)^i A_i sin(\omega(t\text{–}(2i+1)H/V)) \tag{8}$$

where A_i represents the displacement amplitude of the i^{th} seismic wave reflected to the ground surface, and it can be expressed as

$$A_i = \left|\beta^{\frac{T_g}{T}} R_e\right|^i A_0 \tag{9}$$

Eqs. (6)–(8) represent the displacement of the upward-propagating waves at the ground surface. The displacement of the ground surface equals the sum of those of the upward- and downward-propagating waves at the ground surface. Eq. (3) implies that the upward-propagating incident wave and the downward-propagating reflected wave at the ground surface have the same displacement and polarity. Thus, the displacement of the ground surface induced by the i^{th} seismic wave reflected back to the ground surface is $2y_i\,(t)$. For an infinite incident seismic wave, all the seismic waves reflected back to the ground surface exist at the ground surface simultaneously; hence, the displacement of the ground surface, $y_S(t)$, can be expressed as

$$y_S(t) = \sum_{i=0}^{\infty} 2y_i(t) \tag{10}$$

Similarly, the displacement of the outcrop bedrock, $y_B(t)$, can be expressed as

$$y_B(t) = 2Asin(\omega t) \tag{11}$$

Then, to obtain the response spectral ratio of the single-layer soil model, the response spectra on the ground surface and outcrop bedrock should be derived. As shown in Fig. 2(b), because displacement $y_B(t)$ of the outcrop bedrock is a sinusoidal function, if the transient response is ignored, the corresponding response spectrum, $RS_B(\omega, \bar{\omega}, h_0)$, can be easily obtained as

$$RS_B(\omega, \bar{\omega}, \mathrm{h}_0) = 2AH_0(\omega, \bar{\omega}, \mathrm{h}_0) \tag{12}$$

where $H_0(\omega, \bar{\omega}, h_0)$ is the displacement transfer function for a single-degree-of-freedom (SDOF) structure (Fig. 2(b)) with circular frequency $\bar{\omega}$ and damping ratio h_0, and it can be expressed as

$$H_0(\omega, \bar{\omega}, \mathrm{h}_0) = \frac{\omega^2}{\sqrt{(2\mathrm{h}_0\omega\bar{\omega})^2 + (\omega^2 - \bar{\omega}^2)^2}} \tag{13}$$

The displacement of the ground surface equals the sum of a series of sinusoidal functions with the same circular frequency ω but different phases, $\omega(t\text{–}(2i+1)H/V)$, as indicated by Eqs. (8) and (10). According to the algorithms of a trigonometric function, the displacement of the ground surface eventually develops into a sinusoidal function. Similarly, the displacement response spectrum on the ground surface, $RS_S(\omega, \bar{\omega}, h_0)$, can be expressed as

$$RS_S(\omega, \bar{\omega}, \mathrm{h}_0) = A_S(\omega)H_0(\omega, \bar{\omega}, \mathrm{h}_0) \tag{14}$$

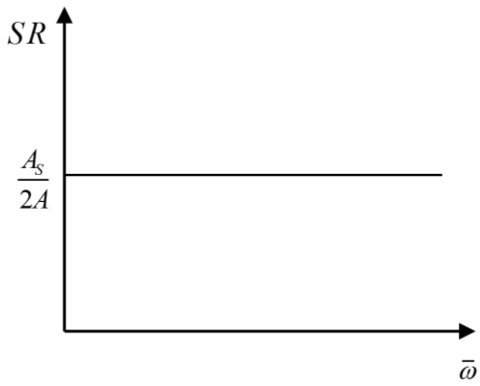

Fig. 3 Response spectral ratio of a single-layer soil profile subjected to a harmonic seismic wave

where $A_S(\omega)$ is the displacement amplitude of the ground surface. Due to the one-dimensional approximation applied in the soil model (Fig. 2(a)), i.e., the infinite extension and same movement of the soil layer in the horizontal direction, the mass and rigidity of the soil medium are infinite relative to the structural system. Therefore, such simple soil and structure models cannot incorporate the soil-structure interaction. The soil-structure interaction effect can be considered separately by adjusting the structural parameters (e.g., adding the damping ratio and changing the first period) in practical seismic design (ASCE/SEI 7-10, 2011). Similar to the general response spectra, $RS_B(\omega, \bar{\omega}, h_0)$ and $RS_S(\omega, \bar{\omega}, h_0)$ are functions of the oscillator circular frequency $\bar{\omega}$ and damping ratio h_0, respectively. Equation (13) indicates that if circular frequency ω of the incident wave is considered as a variable, then $RS_B(\omega, \bar{\omega}, h_0)$ and $RS_S(\omega, \bar{\omega}, h_0)$ are also functions of circular frequency ω. Note that frequencies ω and $\bar{\omega}$ are physically different, i.e., ω is the circular frequency of the seismic motion and $\bar{\omega}$ is the oscillator circular frequency.

By dividing the ground-surface response spectrum (Eq. (14)) by the outcrop-bedrock response spectrum (Eq. (12)), the response spectral ratio can be obtained as

$$SR(\omega) = \frac{A_S(\omega)}{2A} \tag{15}$$

Eq. (15) indicates that for harmonic incident seismic waves, the response spectral ratio is the same as the displacement–amplitude ratio of the ground-surface motion with respect to outcrop-bedrock motion when the transient response is ignored. In addition, Eq. (15) indicates that although both the response spectra on the ground surface and outcrop bedrock are functions of the oscillator circular frequency $\bar{\omega}$ and damping ratio h_0, the response spectral ratio is independent of these two parameters. This implies that for a specific harmonic incident seismic wave, the response spectral ratio of a single-layer soil profile is constant and equals $\frac{A_S}{2A}$, as illustrated in Fig. 3. However, the response spectral ratio is dependent on circular frequency ω because displacement amplitude $A_S(\omega)$ of the ground surface is dependent on ω, as indicated by Eqs. (8) and (10). In other words, the response spectral ratio varies with the incident seismic motion, even in the case of the linear analysis of a specific soil profile. Zhao *et al*. (2009, 2010) had determined the same phenomenon through the statistical analysis of actual seismic records, and Stafford *et al*. (2019) provided a reasonable explanation for the phenomenon based on the random vibration theory. Here, Eq. (15) can provide theoretical support for this phenomenon. In addition, comparing with the well-known transfer function of the single-layer soil model, Eq. (15) is much easier to understand and apply for the derivation of an SR_{Tg} equation for practical seismic design, as will be detailed below.

2.2 Formulation of SR_{Tg} for practical seismic design

To obtain soil displacement-response spectra based on the bilinear model, the calculation of the response spectral ratio at the site fundamental period SR_{Tg} is an essential step, as introduced earlier. For harmonic seismic waves, SR_{Tg} can be easily determined by Eq. (15) using the impedance ratio, soil damping ratio, and the circular frequency of the bedrock seismic motion. However, for practical seismic design considering real seismic waves, the determination of SR_{Tg} is much more complicated. Even for the simple single-layer soil model, SR_{Tg} needs to be obtained by site response analyses, and there is not an explicit solution for real seismic waves up to now. This section aims to propose a simple and explicit SR_{Tg} formulation for practical seismic design.

For real seismic waves, SR_{Tg} is affected not only by parameters of the soil profile but also by seismological parameters determining the bedrock seismic motion, for example, the magnitude, source-to-site distance, and source type, even for linear analysis (Zhao *et al*. 2009, 2010, Stafford *et al*. 2017, Zhang and Zhao 2021a, b). In principle, all these soil and seismological parameters should be included in the SR_{Tg} formulation. However, the seismological parameters are generally not available in seismic codes when the response spectrum is adopted as the seismic load for structural design. Therefore, it is necessary to find another approach to incorporate the effects of the seismological parameters into the SR_{Tg} formulation. Zhao *et al*. (2009, 2010), Stafford *et al*. (2017), and Zhang and Zhao (2021a, 2021b) have theoretically and statistically determined that for real seismic waves, SR_{Tg} generally increases with increasing magnitude and approaches the Fourier spectral ratio at the site fundamental period, i.e., the maximum value of SR_{Tg} for harmonic seismic waves. This phenomenon is also confirmed in the following text. In addition, earthquakes with large magnitudes are generally considered in seismic design particularly in high-seismicity regions. To simply consider the SR_{Tg} variation with respect to the seismological parameters, the maximum value of SR_{Tg} for harmonic seismic waves is proposed as the design value in this study. Hence, regardless of the SR_{Tg} variation with respect to bedrock seismic motions, the design value for SR_{Tg} will always be conservative and reasonable for seismic design in high-seismicity regions.

According to Eq. (15), to obtain the maximum response spectral ratio, the maximum displacement amplitude of the ground surface should be obtained. Equation (10) indicates that displacement amplitude $A_S(\omega)$ of the ground surface is determined by the amplitude and phase of each sinusoidal function, which is dependent on circular frequency ω. If the phase difference between the i^{th} and $(i+1)^{th}$ sinusoidal functions $(\frac{2H\omega}{V})$ is $(2n-1)\pi$ (n = 1, 2, 3…), that is, if circular frequency ω of the incident wave satisfies

$$\omega = \frac{(2n-1)\pi V}{2H} \tag{16}$$

then Eq. (10) can be rewritten as

$$y_S(t) = \sum_{i=0}^{\infty} 2A_i sin(\omega(t - H/V)) \tag{17}$$

Hence, the maximum and minimum of each sinusoidal function is achieved simultaneously. In addition, as displacement amplitude A_i of each sinusoidal function decreases with an increase in circular frequency ω, as indicated by Eq. (9), if n = 1 in Eq. (16), displacement amplitude $A_S(\omega)$ of the ground surface will reach its maximum, and thus response spectral ratio $SR(\omega)$ is maximized. According to Eqs. (9) and (17), the maximum amplitude of the ground surface, $A_{S\bullet max}(\omega)$, is twice the sum of the amplitude of each sinusoidal function, and it can be expressed as

$$A0\sum_{i=0}^{\infty}|\beta R_e|^i \quad Smax \\ = 2A_0(1-\beta R_e + (\beta R_e)^2 - (\beta R_e)^3 + \ldots) \tag{18}$$

In Eq. (18), the infinite sum within brackets has a well-established value, which corresponds to the following series:

$$(1+x)^{-1} = 1 - x + x^2 - x^3 + \ldots (x^2 < 1) \tag{19}$$

where $x = \beta R_e$. The convergence condition, $x^2 < 1$, is automatically satisfied in this case. Finally,

$$A_{S\text{·max}}(\omega) = 2A_0(1+\beta R_e)^{-1} \tag{20}$$

By substituting Eqs. (3), (5), and (20) into Eq. (15), the maximum response spectral ratio for the single-layer soil profile subjected to harmonic seismic waves can be obtained as

$$SR_{Tg} = \frac{2I\beta^{1/2}}{(1+I)+(1-I)\beta} \tag{21}$$

Eq. (21) provides an analytical expression of SR_{Tg} for the single-layer soil model. Note that when n = 1 in Eq. (16), the period of the incident wave is equal to site fundamental period T_g, and results in the resonance between the incident seismic wave and soil profile. Thus, Eq. (21) represents the soil resonance effect. In addition, because the response spectral ratio is the same as the displacement–amplitude ratio for harmonic incident seismic waves, Eq. (21) also represents the maximum amplification ratio of the displacement amplitude.

Eq. (21) is derived based on a single-layer soil model, for the estimation of actual multi-layer soil sites, the multiple soil layers are approximated to a single layer with an equivalent shear wave velocity V_{eq} expressed by

$$V_{eq} = \frac{\sum_{k=1}^{n} H_k}{\sum_{k=1}^{n} \frac{H_k}{V_k}} \tag{22}$$

where, k is the layer number. If one needs to fully incorporate the shear wave velocity profile, more elaborate approaches for estimating the equivalent shear wave velocity can be used, e.g., the one in the building code of Mexico (Aviles and Perez-Rocha 2012) or that by Zhang and Zhao (2018) and Zhang and Zhao (2017).

2.3 Justification of the maximum-value approximation

In Section 2.2, the maximum value of SR_{Tg} for harmonic seismic waves is adopted as the design value of SR_{Tg} for actual seismic waves. The rationality of this proposal is further discussed in this section. As is known, any seismic wave f (t) can be expressed as the sum of a series of hormonal waves based on the Fourier transform,

$$f(t) = \frac{1}{2}a_0 + \sum_{k=1}^{+\infty} a_k \, sin(\, \omega_k t + \varphi_k) \tag{23}$$

where a_k and φ_k (k = 1,2…) represent the amplitude and phase lag of the component with a circular frequency of ω_k, respectively. The response spectrum of the seismic wave at an oscillator period $\bar{T}$ ($\bar{T} = \frac{2\pi}{\bar{\omega}}$) is largely affected by the components in the seismic wave with periods around $\bar{T}$ ($T \approx \bar{T}$), even these components are not predominant in the seismic wave. Because the SDOF system acting as a narrowband filter amplifies the components near the oscillator period $\bar{T}$ (10 times for 5% damping) much more significantly comparing with those at other periods. Hence, for the single-layer soil profile subjected to an actual seismic wave, the response spectra at the site fundamental period, T_g, ($\bar{T} = T_g$) on the ground surface and outcrop bedrock are largely affected by the corresponding components in the seismic waves with periods around T_g ($T \approx T_g$). Therefore, the response spectral ratio, SR_{Tg}, at site fundamental period T_g is close to the site amplification ratio for the T_g-period component ($T = T_g$), i.e., the maximum value of SR_{Tg} for harmonic seismic waves expressed by Eq. (21). Although other components except those with T_g in the seismic waves also contribute to the response spectrum at T_g, their site amplification ratios with periods other than T_g in the seismic wave are all smaller than those obtained using Eq. (21). This is because Eq. (21) represents the maximum amplification ratio of the displacement amplitude. Hence, the site-amplification ratio for the sum of all components in the seismic wave that contribute to the response spectrum at T_g, that is, SR_{Tg} for the actual seismic wave is typically smaller than that determined using Eq. (21). This implies that Eq. (21) can provide a conservative estimation of SR_{Tg} for actual seismic waves. In addition, as introduced above, recent studies (Zhao *et al.* 2009, 2010, Stafford *et al.* 2017, Zhang and Zhao 2021a, b) have proved

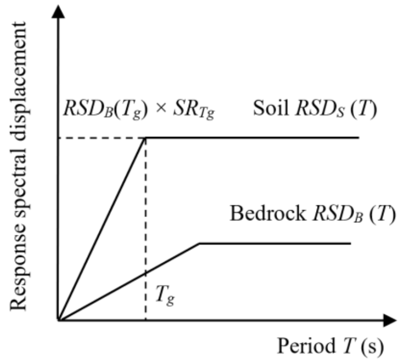

Fig. 4 Construction of a soil displacement-response spectrum for seismic design

that for real seismic waves, SR_{Tg} generally increases with increasing magnitude and approaches the maximum value of SR_{Tg} for harmonic seismic waves. Therefore, the maximum-value approximation is reasonable for cases with large magnitudes considered for seismic design particularly in high-seismicity regions. The rationality of this approximation is further verified in the next section.

2.4 Soil-displacement spectra

The proposed equation for SR_{Tg} (Eq. (21)) can directly be applied to constructing the soil displacement-response spectrum, RSD_S, based on the bilinear model, as shown in Fig. 4. First, the bedrock displacement-response spectrum, RSD_B, should be estimated. For regions where the bedrock displacement-response spectrum, RSD_B, is achieved in the seismic codes, the RSD_B corresponding to the specified hazard level can be obtained directly. Further, for regions where the bedrock displacement-response spectrum is not defined in the seismic codes, it can be obtained using seismic motion-prediction models, such as those developed by Lam *et al.* (2000a, b). Then, by using the derived equation for SR_{Tg}, the soil displacement-response spectrum at the site fundamental period, i.e., $RSD_S(T_g)$, can be obtained as

$$RSD_S(T_g) = RSD_B(T_g) \times SR_{Tg} \tag{24}$$

where $RSD_B(T_g)$ is the bedrock displacement-response spectrum at the site fundamental period. After obtaining $RSD_S(T_g)$, the soil displacement-response spectrum over the entire period can be constructed using two straight lines, as shown in Fig. 4. In addition, the nonlinear behavior of soil, including the degradation of the shear wave velocity and increase in the soil damping ratio, can be considered by using, for example, the method in (Tsang *et al.* 2006b). Note that although the maximum amplification ratio, SR_{Tg}, is used to reflect the site resonance effect, soil-amplification ratios for displacement spectra at all periods are not necessarily equal to SR_{Tg}. As observed in Fig. 4, the soil-amplification ratios for the displacement spectra at periods longer than T_g are all smaller than SR_{Tg}.

In addition, note that with the use of the bilinear model, the maximum displacement spectrum remains constant over the entire long-period range. This does not conform to the

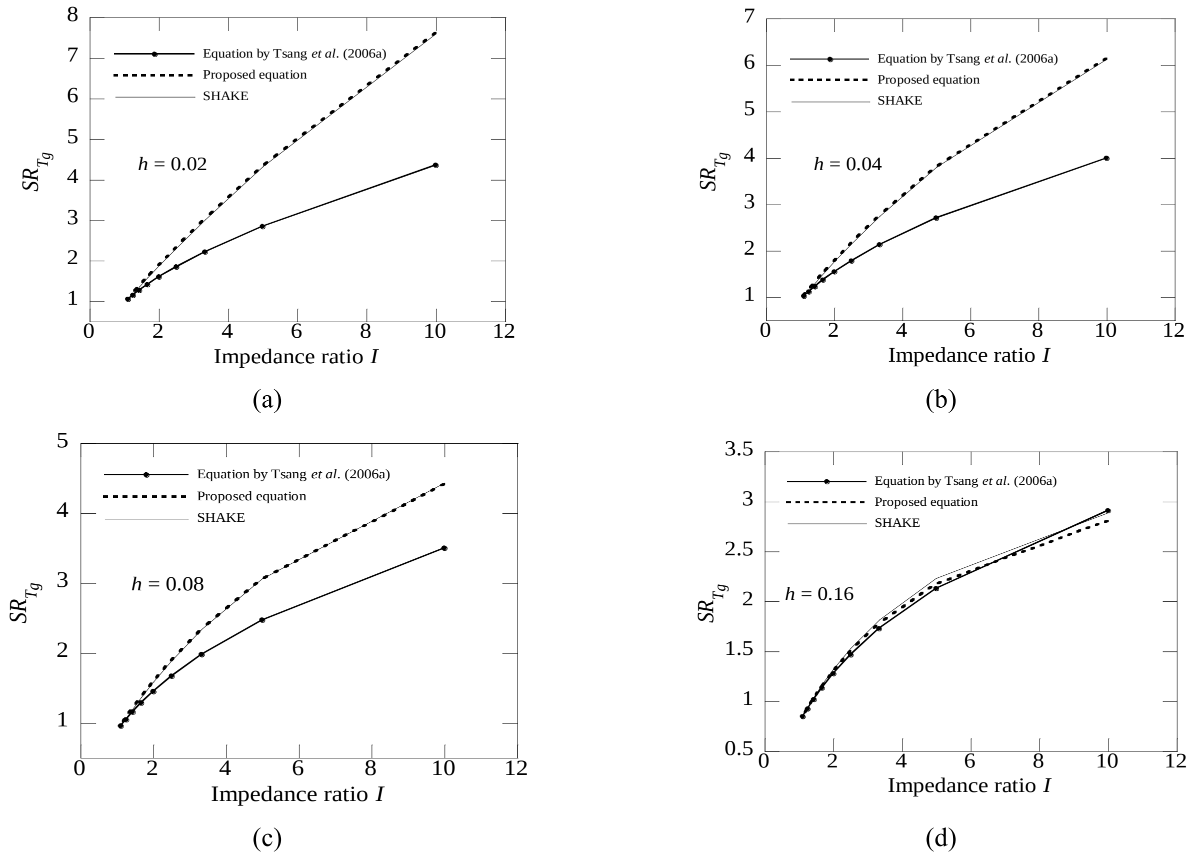

Fig. 5 Comparisons of SR_{Tg} values obtained by the proposed equation, SHAKE program, and the equation by Tsang *et al.* (2006a), considering harmonic seismic waves at (a) h = 0.02, (b) h = 0.04, (c) h = 0.08, and (d) h = 0.16

Table 1 Characteristics of the created sites

Name	Site 1	Site 2	Site 3	Site 4	Site 5	Site 6	Site 7	Site 8	Site 9	Site 10
H (m)	7.5	15	37.5	75	150	7.5	15	37.5	75	150
V (m/s)					300					
V_B (m/s)			600					1500		

characteristics of the observed displacement spectrum, which decreases from a certain period and converges to the peak ground displacement for a sufficiently long period. By using the bilinear model, the displacement spectra over long periods could be overestimated. Nevertheless, the corner period, at which the displacement spectrum begins to decrease, is generally very long. For example, for the soil-displacement spectra (ground types B–E) defined in Eurocode 8, corner periods are all longer than 5 s, and this is supported by the results derived from many statistical studies (Tolis and Faccioli 1999, Guan *et al.* 2004). Therefore, the proposed bilinear model can be applied for estimating the displacement spectrum up to 5 s.

3. Verification of the proposed model

3.1 Verification of SR_{Tg} considering harmonic seismic waves

The equation for SR_{Tg}, i.e., Eq. (21), is derived based on the harmonic incident wave with a period equal to the site fundamental period, introduced earlier. To confirm the validity of the derived equation, the obtained results were compared with those obtained using the SHAKE program, considering the same harmonic incident wave. The SHAKE program is a robust analysis tool, proven by its extensive use over some 40 years. Since the SHAKE program is limited to the calculation of time histories and Fourier spectra, the response spectra, response spectral ratios, and SR_{Tg} need to be further calculated using the obtained time histories. A range of single-layer soil profiles on bedrock were considered; impedance ratio I of bedrock-to-soil layer ranges from 1 to 10, and damping ratio h of the soil layer ranges from 0.02 to 0.16. Fig. 5 shows the comparison of the results calculated by the derived equation and SHAKE program. The results obtained by the derived equation were found to agree considerably well with those obtained through the SHAKE program for nearly all the considered cases. Although the accuracy decreases with increasing soil damping ratio h, the maximum relative error is only 4% even for h = 0.16, as shown in Fig. 5(d). The good

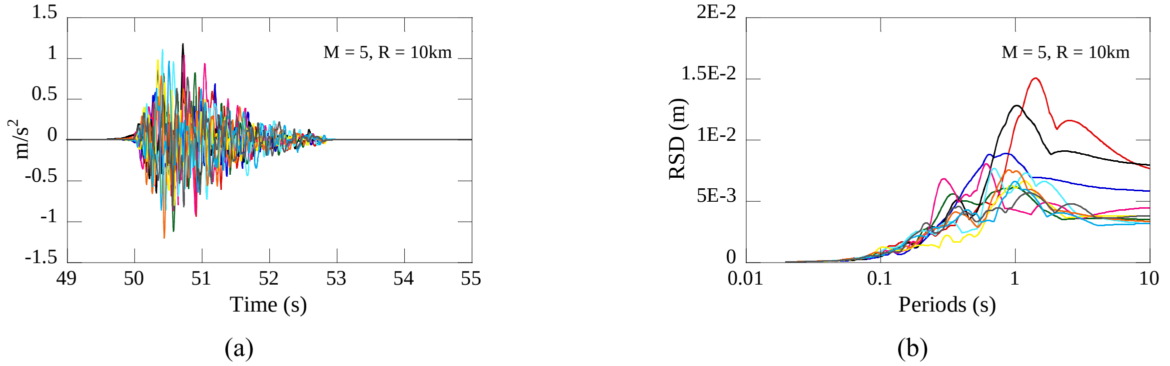

Fig. 6 Simulated (a) acceleration time histories and (b) displacement response spectra based on the stochastic method (Boore 1983, 2003)

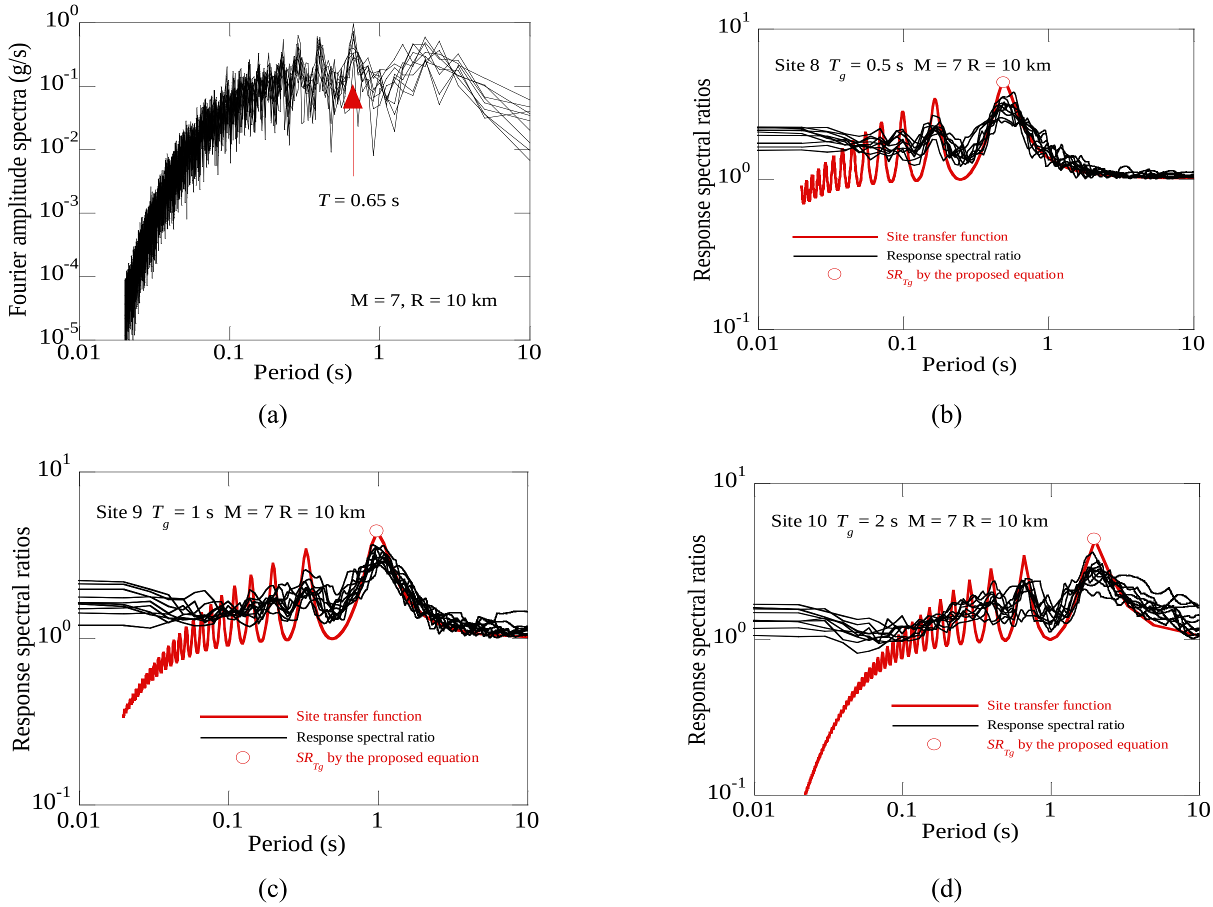

Fig. 7 (a) Fourier amplitude spectra, and response spectral ratios for (b) site 8, (c) site 9, and (d) site 10

agreement between the results by Eq. (21) and the SHAKE program is because Eq. (21) is an accurate solution of SR_{Tg} for harmonic seismic waves under the conditions described in Sections 2.1 and 2.2.

The results obtained using the equation of Tsang *et al.* (2006*a*) are also plotted in Fig. 5. As observed, the equation provides a lower value of SR_{Tg} for many cases, especially for those with a large impedance ratio and small soil damping ratio, as shown in Figs. 5 (a)-5(c). However, for the cases with a large soil damping ratio, as shown in Fig. 5(d), the equation in Tsang *et al.* (2006*a*) provides a good estimation of SR_{Tg} and yields results similar to those obtained using the proposed equation (Eq. (21)).

3.2 Verification of SR_{Tg} by considering recorded and synthetic earthquake motions

To further verify whether the proposed SR_{Tg} equation is suitable for general seismic waves, it was compared with the SHAKE program using recorded and synthetic earthquake motions. For this purpose, 10 single-layer soil profiles on bedrock were created. Thickness H of the soil

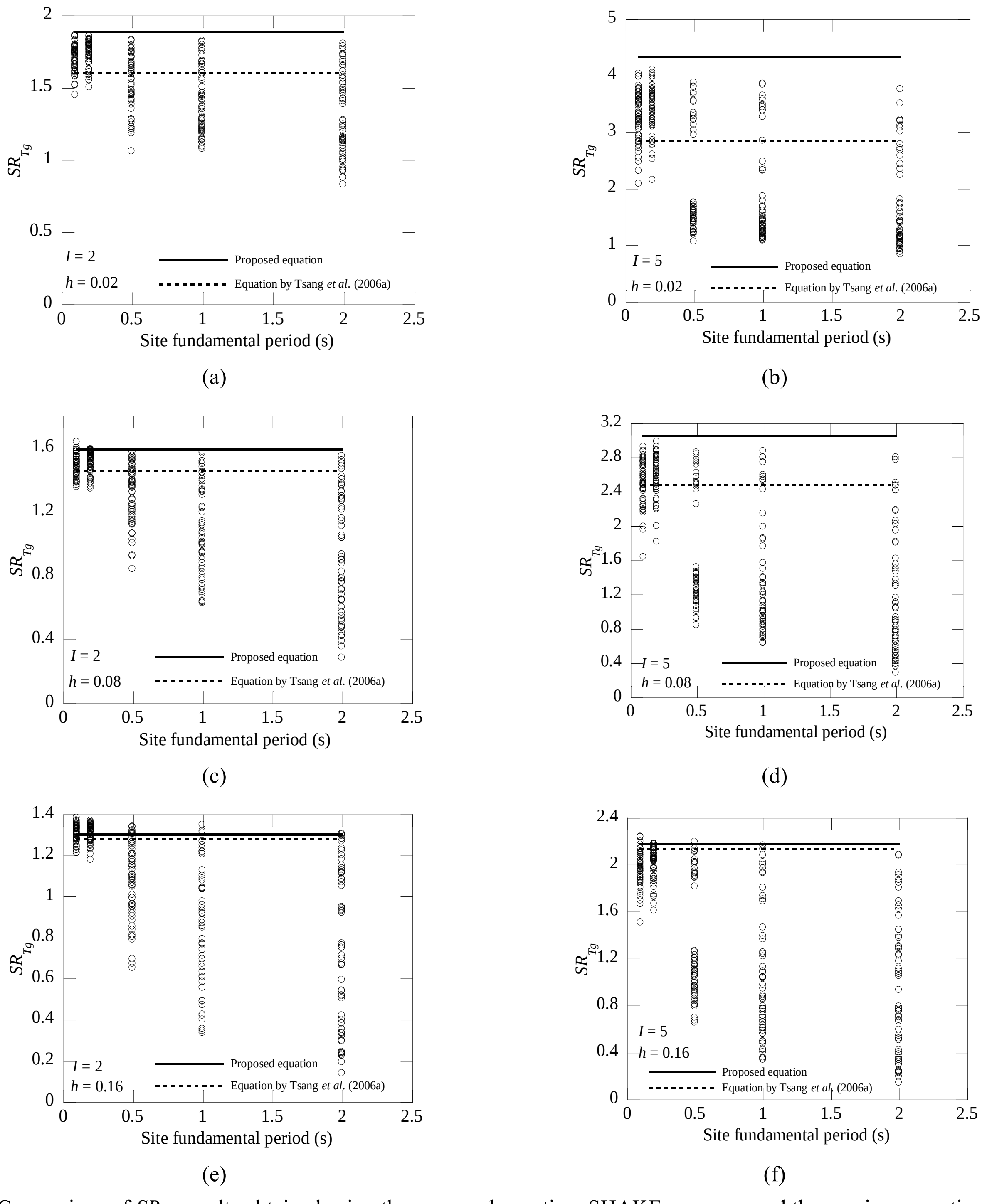

Fig. 8 Comparison of SR_{Tg} results obtained using the proposed equation, SHAKE program, and the previous equation (Tsang *et al*. 2006a), considering recorded earthquake motions for (a) $I = 2$, $h = 0.02$; (b) $I = 5$, $h = 0.02$; (c) $I = 2$, $h = 0.08$; (d) $I = 5$, $h = 0.08$; (e) $I = 2$, $h = 0.16$; and (f) $I = 5$, $h = 0.16$

layer and shear-wave velocity of the rock half-space V_B varied widely, as summarized in Table 1. The shear-wave velocity of the soil layer was set to V = 300 m/s. The damping ratio of the soil layer was verified to range from h = 0.02 to 0.16, and the damping ratio of the bedrock was set to zero. The 10 created soil profiles are labeled as sites 1-10, as listed in Table 1. The impedance ratio of the bedrock-to-soil layers was calculated as $I = 2$ for sites 1-5, and $I = 5$ for sites 6-10. The undamped fundamental period of the sites ranges from 0.1 s for the shallowest site to 2 s for the deepest site.

Then, 56 earthquake motions recorded on rock sites were selected from the Strong-motion Seismograph Network (K-NET, KiK-net) of Japan. To control the signal-to-noise ratio, the earthquake motions that with peak accelerations above 5 gal were selected. The magnitude of

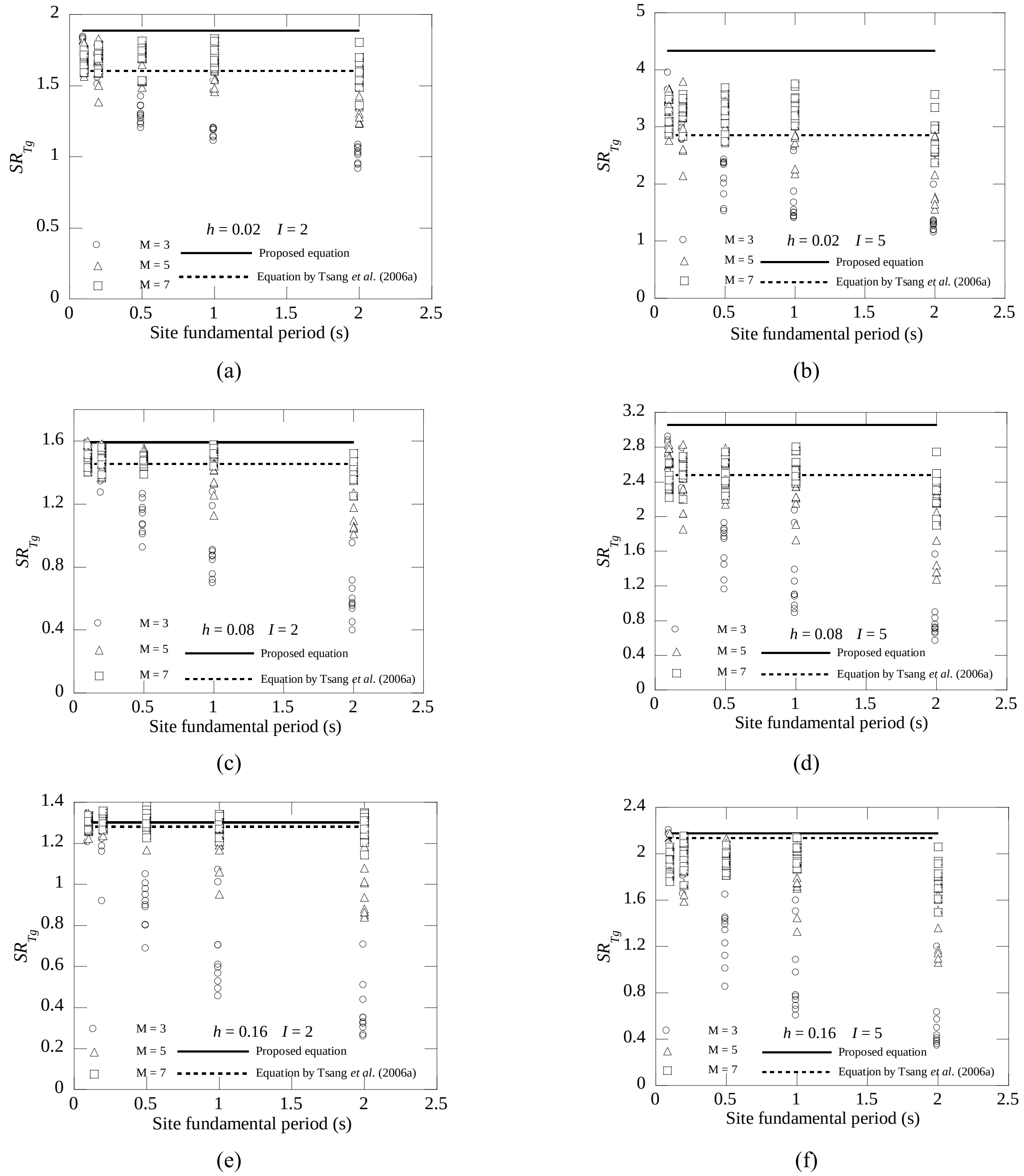

Fig. 9 Comparison of SR_{Tg} results obtained using the proposed equation, SHAKE program, and previous equation (Tsang *et al*. 2006a), considering synthetic earthquake motions generated through stochastic simulations for (a) $I = 2$, $h = 0.02$; (b) $I = 5$, $h = 0.02$; (c) $I = 2$, $h = 0.08$; (d) $I = 5$, $h = 0.08$; (e) $I = 2$, $h = 0.16$; and (f) $I = 5$, $h = 0.16$

the selected earthquake motions varied widely from 2.8 to 6.1, and the epicentral distance varied widely from 7 to 241 km. In addition, to confirm the trend of SR_{Tg} with variations in the magnitude of the ground motion mentioned earlier, ground motions with similar characteristics but different magnitudes were generated using a stochastic method (Boore 2003). To generate such ground motions, Fourier amplitude spectra (FAS) were first generated by the stochastic-method simulation (SMSIM) program (Boore 2015) using a single-corner-frequency source spectrum. The ground-motion model using this source spectrum is easy to apply and has been validated by comparison with observations from actual seismic records (Boore 2003). The important seismological parameters describing the FAS of the input motion were determined according to the method presented by Boore (2003). A fixed distance of 10 km and three magnitudes of M = 3.0, 5.0, and 7.0 were considered for generating the FAS. The earthquake time history was then generated from the FAS by using the SMSIM program (Boore 2015) through a stochastic simulation (Boore 1983,

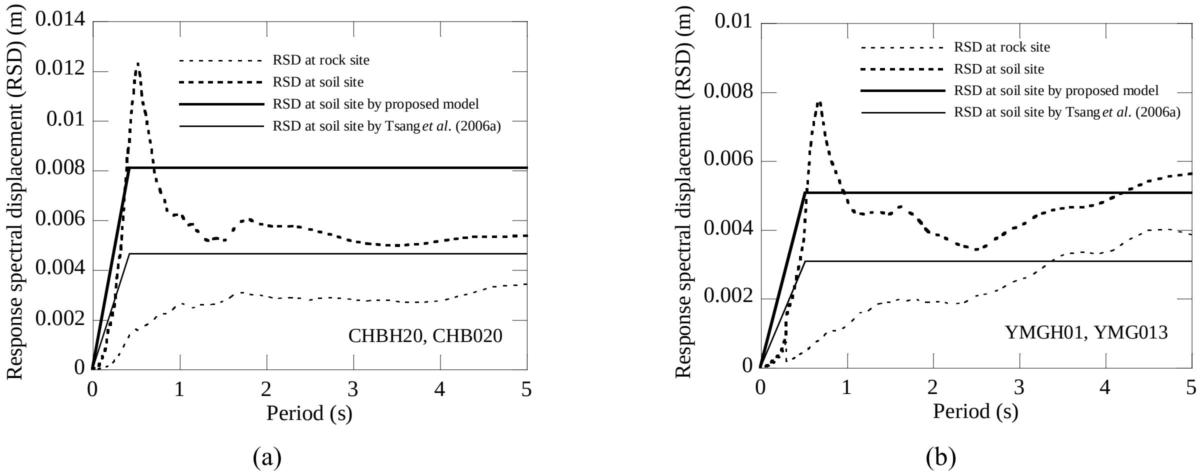

Fig. 10 Comparisons of soil displacement-response spectra obtained from recorded ground motions, the proposed model, and the model in Tsang *et al*. (2006a) for soil sites (a) CHB020 and (b) YMG013

2003). The duration of the time histories was determined according to the method proposed in Atkinson and Silva (2000). For each FAS, a suite of 10 time histories was generated, and the simulated time histories match the FAS on average. Fig. 6 shows the simulated acceleration time histories and corresponding displacement response spectra for M = 5.0 and R = 10 km.

Then, response spectral ratios are calculated by the SHAKE program considering the recorded and synthetic earthquake motions. Fig. 7 shows some representative results of the synthetic earthquake motions. Fig. 7(a) shows FAS of the input motions; Figs. 7(b)-7(d) shows calculated response spectral ratios. Figs. 8 and 9 show the comparison of SR_{Tg} results calculated using the derived equation and SHAKE program. In the figures, the solid lines represent the results of the derived equation (Eq. (21)), and the circles, triangles, and squares represent the results of the SHAKE program. The left panels of Fig. 8 and 9 (panels (a), (c), and (e)) show the results of sites 1–5 with an impedance ratio of 2, and the right panels (panels (b), (d), and (f)) show the results of sites 6–10 with an impedance ratio of 5. The three rows represent the results of different soil damping ratios. Note that the values of SR_{Tg} obtained using the SHAKE program vary significantly relative to impedance ratio I, soil damping ratio h, and the site fundamental period; however, most results do not exceed those obtained using Eq. (21). Eq. (21) may slightly underestimate SR_{Tg} only for a few cases with small impedance ratios and large soil damping ratios, as shown in Figs. 8(e) and 9(e). These conclusions support the discussion in Sections 2.2 and 2.3. In addition, SR_{Tg} varies significantly with the magnitude of the bedrock motion even for the linear analysis of a specific site; it generally increases with increasing magnitude, as shown in Fig. 9. This phenomenon has already been discussed in many previous studies (Zhao *et al*. 2009, 2010, Stafford *et al*. 2017, Zhang and Zhao 2021a, b). Zhao and Zhang (2009) named the effect of bedrock motions as "side effect." The proposed equation may provide overly conservative estimations for the cases with small magnitudes, but it provides reasonable estimations for those with moderate and large magnitudes. In seismic design, the seismic load generally corresponds to relatively large magnitudes for the ultimate limit state design, particularly in high-seismicity regions. Hence, the equation is considered suitable for seismic design in high-seismicity regions.

In addition, the results obtained using the equation by Tsang *et al*. (2006a) are presented in Figs. 8 and 9 and represented by dotted lines. Their equation yields lower values of SR_{Tg}, especially in the case of large magnitudes and large impedance ratios, small soil damping ratios, and short site fundamental periods. However, for the cases with large soil damping ratios, as shown in Figs. 8(e), 8(f), 9(e), and 9(f), their equation (Tsang *et al*. 2006a) and the equation derived in the current study yield similar results and provide a conservative estimation of SR_{Tg}. In general, Eq. (21) can provide a conservative and reasonable estimation of SR_{Tg} in most cases for both recorded and synthetic earthquake motions, particularly for cases with large magnitudes.

3.3 Verification of soil displacement-response spectra

In this section, the model developed for the construction of soil displacement-response spectra is verified. For the verification, we selected two pairs of nearby soil and rock sites from K-NET and KiK-net, due to such sites are very limited. For these two pairs of rock and soil sites, the distances from the rock to the soil site were 3.04 and 0.02 km, respectively. The station codes of the rock (CHBH20 and YMGH01) and soil sites (CHB020 and YMG013) are presented in Fig. 10. Ground motions are selected that are from the same earthquakes and recorded simultaneously at both the rock and nearby soil sites. To control the signal-to-noise ratio, the ground motions with peak accelerations above 5 gal were selected. To reduce the path effect on the response spectrum, ground motions with epicentral distances of more than 10 times the distance between the rock and soil sites were selected; as such, 60 recorded ground motions were selected in total. Then, the

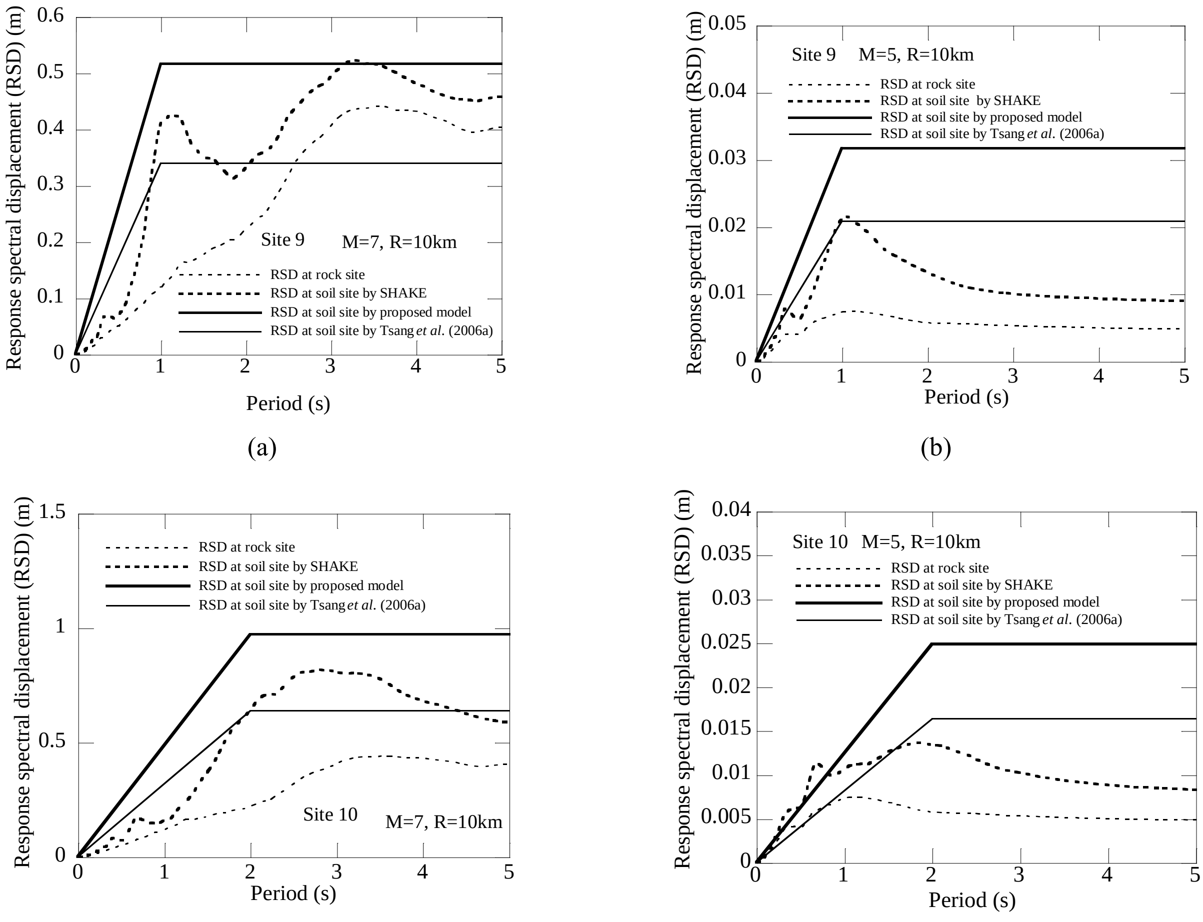

Fig. 11. Comparisons of soil displacement-response spectra obtained by the proposed model, SHAKE program, and the model in Tsang *et al.* (2006a) considering synthetic earthquake motions generated by stochastic simulation for (a) Site 9, M = 7, R = 10 km; (b) Site 9, M = 5, R = 10 km; (c) Site 10, M = 7, R = 10 km; and (d) Site 10, M = 5, R = 10 km

displacement response spectra of the ground motions on the rock and soil sites were calculated and averaged. The averaged soil displacement-response spectrum is compared with that calculated by the proposed model according to the averaged bedrock-response spectrum, as shown in Fig. 10. In addition, to investigate the variation in the accuracy of the proposed model in terms of magnitude, the 10 bedrock and soil-surface-response spectra simulated at each site in terms of magnitude were averaged. The representative comparisons of the soil response spectra obtained using the proposed model and SHAKE program are shown in Fig. 11.

As such, the proposed model was determined to generally provide a good estimation of the soil displacement-response spectrum for most actual and simulated sites. The average error of soil displacement-response spectra at periods between 0 ~ 5 s by the proposed model is around 18% compared to the results of real seismic records in Fig. 10. For the simulated single-layer soil sites (Fig. 11), the proposed model provided conservative estimations in almost all the cases. Although the proposed model may provide overly conservative estimations in cases with small magnitudes, as shown in Figs. 11(b) and (d), it provides reasonable estimations for those with large magnitudes, as shown in Figs. 11(a) and (c). The latter case is typically considered for seismic design for the ultimate limit state particularly in high seismicity regions. This conclusion is consistent with that for the SR_{Tg} obtained in section 3.2. For the two actual soil sites (Fig. 10), because of the complexities involved in an actual situation, the proposed model underestimates the results around the peak (possibly owing to the single-layer approximation (Zhang and Zhao 2017, 2018)) but provides good estimations of the overall results at most periods. In addition, the results obtained using the model in Tsang *et al.* (2006a) are also presented in Figs. 10 and 11. As observed, for the created single-layer soil sites, the model in Tsang *et al.* (2006a) may produce lower values of response spectra for the cases with large magnitudes, whereas for the actual sites, the underestimation is more significant.

4. Conclusions

The displacement-response spectrum, as the seismic input, is of great significance to performance-based seismic designs. This paper presented a convenient and efficient model for the construction of displacement-response spectra considering the soil-resonance effect. Applying the proposed model, one only needs to calculate SR_{Tg}, then by using the bilinear model, a soil displacement-response spectrum can be easily constructed. The whole calculation can even be implemented using hand without any software. Even with such a simple model, the predicted results agree very well with those from actual observations and SHAKE analyses. This study makes the definition of the displacement-response spectrum more reasonable and promotes the development of a performance-based seismic design. The conclusions derived in this study can be summarized as follows:

• A simple and rational equation for the response spectral ratio at the fundamental period, SR_{Tg}, was proposed based on the analysis of a single-layer soil model using the wave multiple reflection theory.

• By using the proposed equation for SR_{Tg}, a simple approach was presented to construct soil displacement-response spectra based on a bilinear model.

• The proposed model was verified by comparison with results obtained from observations and by using the SHAKE program, considering recorded and synthetic earthquake motions as well as harmonic seismic waves. The results showed that the derived model can lead to good estimations of SR_{Tg} for harmonic incident seismic waves with a relative error of less than 4% and lead to reasonable estimations of both SR_{Tg} and soil displacement-response spectra, for earthquakes with a relatively large magnitude, which are generally considered for seismic design particularly in high-seismicity regions. The average error of soil displacement-response spectra at periods between 0 ~ 5 s by the proposed model is around 18% compared to the results of real seismic records.

Acknowledgments

This study was partially supported by the National Natural Science Foundation of China (Grant No. 1951738001). This support is gratefully acknowledged.

References

Atkinson, G.M. and Silva, W. (2000), "Stochastic Modeling of California Ground Motions", *Bull. Seism. Soc. Am.*, **90**(2), 255-274. https://doi.org/10.1785/0119990064.

Aviles, J. and Perez-Rocha, L.E. (2000), "Revisions to code provisions for site effects and soil-structure interaction in Mexico", *Earthq. Res. Anal. New Front. Seismol.*, 237-254. https://doi.org/10.5772/28555.

Akkar, S. and Bommer, J.J. (2007), "Prediction of elastic displacement response spectra in Europe and the Middle East", *Earthq. Eng. Struct. Dyn.*, **36**(10), 1275-1301. https://doi.org/10.1002/eqe.679.

ASCE/SEI 7-10 (2011), *Minimum Design Loads for Buildings and Other Structures*, American Society of Civil Engineers (ASCE), USA.

Boore, D.M. (1983), "Stochastic simulation of high-frequency ground motions based on seismological models of the radiated spectra", *Bull. Seism. Soc. Am.*, **73**(6A), 1865-1894. https://doi.org/10.1785/BSSA07306A1865.

Boore, D.M. (2003), "Simulation of ground motion using the stochastic method", *Pure Appl. Geophys.*, **160**, 635-676. https://doi.org/10.1007/PL00012553.

Boore, D.M. (2005), *SMSIM-Fortran Programs for Simulating Ground Motions from Earthquakes: Version 2.3*, U.S. Geol. Surv. Open-File Report. OFR 96-80-A, Menlo Park, California.

Bommer, J.J. and Elnashai, A.S. (1999), "Displacement spectra for seismic design", *J. Earthq. Eng.*, **3**(1), 1-32. https://doi.org/10.1080/13632469909350338.

Calvi, G.M. (2019), "On the correction of spectra by a displacement reduction factor in direct displacement-based seismic design and assessment", *Earthq. Eng. Struct. Dyn.*, **48** (6), 678-685. https://doi.org/10.1002/eqe.3159.

Cauzzi, C. and Faccioli, E. (2008), "Broadband (0.05 to 20 s) prediction of displacement response spectra based on worldwide digital records", *J. Seismology*, **12**, 453-475. https://doi.org/10.1007/s10950-008-9098-y.

Devandiran, P., Kamatchi, P., Balaji Rao, K., Ravisankar, K. and Lyer, N.R. (2013), "Probabilistic analysis of spectral displacement by NSA and NDA", *Earthq. Struct.*, **5**(4), 439-459. http://dx.doi.Org/10.12989/eas.2013.5.4.439.

European Committee for Standardization CEN (2004), *Eurocode 8: design of structures for earthquake resistance-part 1: general rules, seismic actions and rules for buildings*, European Standard EN 1998–1:2004.

Faccioli, E., Paolucci, R. and Rey, J. (2004), "Displacement spectra for long periods", *Earthq. Spectra*, **20**, 347-376. https://doi.org/10.1193/1.1707022.

Guan, J., Hao, H. and Lu Y. (2004), "Generation of probabilistic displacement response spectra for displacement-based design", *Soil Dyn. Earthq. Eng.*, **24**(2), 149-166. https://doi.org/10.1016/j.soildyn.2003.09.005.

Idriss, I.M. and Sun, J.I. (1992), *SHAKE91: A computer program for conducting equivalent linear seismic response analyses of horizontally layered soil deposits. User's Guide*, University of California, Davis.

Pitilakis, K.D., Anastasiadis, A.I., Kakderi, K.G., Manakou, M.V., Manou, D.K., Alexoudi, M.N., Fotopoulou, S.D., Argyroudis, S.A., and Senetakis, K.G. (2011), "Development of comprehensive earthquake loss scenarios for a Greek and a Turkish city: seismic hazard, geotechnical and lifeline aspects", *Earthq. Struct.*, **2**(3), 207-232. http://dx.doi.org/10.12989/eas.2011.2.3.207.

Lam, N.T.K., Wilson, J.L., Chandler, A.M., and Hutchinson G.L. (2000a), "Response spectral relationships for rock sites derived from the component attenuation model", *Earthq. Eng. Struct. Dyn.*, **29**(10), 1457-1489. https://doi.org/10.1002/1096-9845(200010)29:10<1457::AID-EQE969>3.0.CO;2-Q.

Lam, N.T.K., Wilson, J.L., Chandler, A.M. and Hutchinson G.L. (2000b), "Response spectrum modeling for rock sites in low to moderate seismicity regions combining velocity, displacement and acceleration predictions", *Earthq. Eng. Struct. Dyn.*, **29**(10), 1491-1525. https://doi.org/10.1002/1096-9845(200010)29:10<1491::AID-EQE970>3.0.CO;2-T.

Lam, N.T.K., Wilson, J.L. and Chandler, A.M. (2001), "Seismic displacement response spectrum estimated from the analogy soil amplification model", *Eng. Struct.*, **23**(11), 1437-1452. https://doi.org/10.1016/S0141-0296(01)00049-9.

Lumantarna, E., Wilson, J.L. and Lam, N.T.K. (2012), "Bi-linear displacement response spectrum model for engineering applications in low and moderate seismicity regions", *Soil Dyn. Earthq. Eng.*, **43**, 85-96. https://doi.org/10.1016/j.soildyn.2012.07.006.

Maniatakis, C.A. and Spyrakos, C.C. (2012), "A new methodology to determine elastic displacement spectra in the near-fault region", *Soil Dyn. Earthq. Eng.*, **35**, 41-58.

https://doi.org/10.1016/j.soildyn.2011.10.005.
Manolis, G.D., Makra, K., Dineva, P.S. and Rangelov, T.V. (2013), "Seismic motions in a non-homogeneous soil deposit with tunnels by a hybrid computational technique", *Earthq. Struct.*, **5**(2), 161-205. http://dx.doi.org/10.12989/eas.2013.5.2.161.
Muho, E.V., Qian, J. and Beskos, D.E. (2020), "A direct displacement-based seismic design method using a MDOF equivalent system: application to R/C framed structures", *B. Earthq. Eng.*, **18**, 4157-4188. https://doi.org/10.1007/s10518-020-00857-5.
Ranjan, R. and Kumar, A. (2021), "Forecasting ground movement of Patna Region, India", *Earthq. Struct.*, **20**(5), 487-494. http://dx.doi.org/10.12989/eas.2021.20.5.487.
Stafford, P.J., Rodriguez-Marek, A., Edwards, B., Kruiver, P.P. and Bommer, J.J. (2017), "Scenario dependence of linear site effect factors for short-period response spectral ordinates", *Bull. Seism. Soc. Am.*, **107**(6), 2859-2872. https://doi.org/10.1785/0120170084.
Sisi, A.A., Erberik, M.A. and Askan, A. (2018), "The effect of structural variability and local site conditions on building fragility functions", *Earthq. Struct.*, **14**(4), 285-295. http://dx.doi.org/10.12989/eas.2018.14.4.285.
Strong-motion Seismograph Networks (K-NET, KIK-net), http://www.kyoshin.bosai.go.jp/kyoshin/ (accessed 20.11.26).
Tolis, S.V. and Faccioli, E. (1999), "Displacement design spectra", *J. Earthq. Eng.*, **3**(1), 107-125. https://doi.org/10.1080/13632469909350342.
Tsang, H.H., Adrian, M.C. and Lam, N.T.K. (2006a), "Estimating non-linear site response by single period approximation", *Earthq. Eng. Struct. Dyn.*, **35**, 1053-1076.
Tsang, H.H., Adrian, M.C. and Lam, N.T.K. (2006b), "Simple models for estimating period-shift and damping in soil", *Earthq. Eng. Struct. Dyn.*, **35**(9), 1925-1947. https://doi.org/10.1002/eqe.567.
Tsang, H.H., Wilson, J.L., Lam, N.T.K. and Su, R.K.L. (2017), "A design spectrum model for flexible soil sites in regions of low-to-moderate seismicity", *Soil Dyn. Earthq. Eng.*, 92, 36-45. https://doi.org/10.1016/j.soildyn.2016.09.035.
Zhang, H.Z., Saito, T. and Zhao, Y.G. (2017), "Simple calculation method of seismic motion amplification ratio corresponding to fundamental period", *J. Struct. Constr. Eng. AIJ*, **82**, 597-604. (In Japanese). https://doi.org/10.3130/aijs.82.597.
Zhang, H.Z. and Zhao, Y.G. (2018), "A simple approach for estimating the first resonance peak of layered soil profiles" *J. Earthq. Tsunami*, **12**(1), 185005. https://doi.org/10.1142/S1793431118500057.
Zhang, H.Z. and Zhao, Y.G. (2021a), "Investigation of Relationship Between the Response and Fourier Spectral Ratios Based on Statistical Analyses of Strong Motion Records", *J. Earthq. Tsunami*, **15**(2), 2150008. https://doi.org/10.1142/S1793431121500081.
Zhang, H. and Zhao, Y.G. (2021), "Analytical model for response spectral ratio considering the effect of earthquake scenarios", Bull. Earthq. Eng., **19**(12), 5285-5305. https://doi.org/10.1007/s10518-021-01166-1.
Zhang, H.Z. and Zhao, Y.G. (2021c), "Effect of Radiation Damping on the Fundamental Period of Linear Soil Profiles", *J. Earthq. Eng.*, https://doi.org/10.1080/13632469.2021.1911884.
Zhao, Y.G. and Zhang H.Z. (2017), "A simple approach for the fundamental period of MDOF structures", *Earthq. Struct.*, **13**(3), 231-239. http://dx.doi.org/10.12989/eas.2017.13.3.231.
Zhao, G., Xu, L., Gardoni, P. and Xie, L. (2019), "A new method of deriving the acceleration and displacement design spectra of pulse-like ground motions based on the wavelet multi-resolution analysis", *Soil Dyn. Earthq. Eng.*, **119**, 1-10. https://doi.org/10.1016/j.soildyn.2019.01.008.
Zhao, J.X., Zhang, J. and Kojiro, I. (2009), "Side effect of using response spectral amplification ratios for soil sites-variability and earthquake-magnitude and source-distance dependent amplification ratios for soil sites", *Soil Dyn. Earthq. Eng.*, **29** (9),1262-1273. https://doi.org/10.1016/j.soildyn.2009.02.005.
Zhao, J.X. and Zhang, J. (2010), "Side-effect of using response spectral amplification ratios for soft soil sites-Earthquake source-type dependent amplification ratios", *Soil Dyn. Earthq. Eng.*, **30**(4), 258-269. https://doi.org/10.1016/j.soildyn.2009.12.001.

AG